Title

A detailed three-step protocol for live imaging of intracellular traffic in polarized primary porcine RPE monolayers

Authors

Toops, Kimberly A
Tan, Li Xuan
Lakkaraju, Aparna

Publication Date

2014-07-01

DOI

10.1016/j.exer.2014.05.003

Peer reviewed

Experimental Eye Research 124 (2014) 74–85

Contents lists available at ScienceDirect

Experimental Eye Research

journal homepage: www.elsevier.com/locate/yexer

Methods in eye research

A detailed three-step protocol for live imaging of intracellular traffic in polarized primary porcine RPE monolayers

Kimberly A. Toops [a, b], Li Xuan Tan [a, c], Aparna Lakkaraju [a, b, c, *]

[a] Department of Ophthalmology and Visual Sciences, School of Medicine and Public Health, University of Wisconsin-Madison, Madison, WI, USA
[b] McPherson Eye Research Institute, University of Wisconsin-Madison, Madison, WI, USA
[c] Division of Pharmaceutical Sciences, School of Pharmacy, University of Wisconsin-Madison, Madison, WI, USA

ARTICLE INFO

Article history:
Received 8 March 2014
Accepted in revised form 2 May 2014
Available online 23 May 2014

Keywords:
retinal pigment epithelium
polarized monolayers
organelle traffic
live imaging
culture protocol
gene expression
age-related macular degeneration
retinal diseases

1. Introduction

The retinal pigment epithelium (RPE), a monolayer of cuboidal epithelial cells that sits between the photoreceptors and the choriocapillaris, is the initial site of insult in several inherited and acquired blinding diseases, including Stargardt disease, Best disease and age-related macular degeneration (AMD) (Ambati and Fowler, 2012; Bok, 2005; Rattner and Nathans, 2006). This central role for the RPE in retinal dysfunction is largely due to the many critical functions it performs to ensure healthy vision (Bok, 1993; Strauss, 2005) (Fig. 1): the RPE participates in the visual cycle by recycling retinoids to photoreceptors; RPE melanosomes absorb stray light and improve the quality of the visual image; tight junctions between RPE cells form the outer blood-retinal barrier, which maintains ion and fluid homeostasis within the retina and directs vectorial traffic of nutrients into, and metabolites out of, the retina; the RPE secretes growth factors and extracellular matrix components essential for the maintenance of photoreceptors; the RPE secretes vascular endothelial growth factor (VEGF), which is critical for maintaining the choriocapillaris and secretes pigment epithelial-derived factor (PEDF), which suppresses pathological angiogenesis; and last but not least, the RPE participates in photoreceptor renewal by daily phagocytosis and degradation of shed outer segment tips.

The polarized phenotype of the RPE, with a defined repertoire of proteins on the apical and basolateral membrane domains, is critical for carrying out these essential functions (Fig. 1). The RPE is a post-mitotic tissue with limited regenerative potential; therefore, loss of RPE with a concomitant loss of photoreceptor support functions contributes to vision loss in retinal degenerative diseases such as age-related macular degeneration (AMD) (Fuhrmann et al., 2013). Insight into how early changes in the RPE at a cellular level predispose towards disease requires a robust cell-based model system that is amenable to genetic manipulations and microscopy-based assays. Data from RPE cell lines (ARPE-19, d407 and RPE-J) cannot be directly extrapolated to native tissue because these cells lack essential features like tight junctions (d407), high TER (ARPE-19 and d407) or correct apico-basal localization of key RPE membrane proteins (RPE-J and d407) (reviewed in (Bonilha, 2013; Sonoda et al., 2009)). A significant advance in the field was the development of human fetal RPE cultures, first reported by the Bok laboratory and subsequently by the Miller laboratory (Hu and Bok, 2001; Maminishkis et al., 2006). These cells have since been extensively characterized by many other groups (Ablonczy et al.,

* Corresponding author. Department of Ophthalmology and Visual Sciences, University of Wisconsin-Madison, 1300 University Ave, Medical Sciences 677, Madison, WI 53706, USA. Tel.: +1 608 263 6176; fax: +1 608 262 0479.
E-mail address: lakkaraju@wisc.edu (A. Lakkaraju).

http://dx.doi.org/10.1016/j.exer.2014.05.003

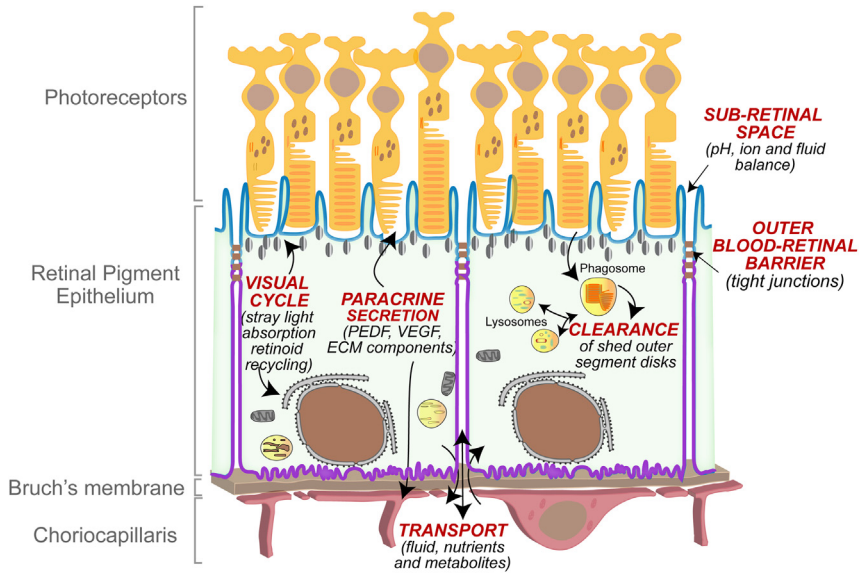

Fig. 1. Functions of the retinal pigment epithelium (RPE) within the retina. The RPE is the outermost layer of the retina and sits beneath the photoreceptors. The Bruch's membrane is a thin extracellular matrix that is located between the RPE and the choroidal blood vessels. RPE cells are polarized with distinct apical (blue) and basolateral (purple) membrane domains demarcated by tight junctions, which form the outer blood-retinal barrier. The RPE directs vectorial transport into the out of the retina and maintains the ionic, pH and fluid balance of the sub-retinal space. The RPE secretes growth factors, hormones, extracellular matrix components (ECM) to maintain photoreceptors, the Bruch's membrane and the choriocapillaris. RPE cells participate in the visual cycle by recycling retinoids and melanosomes improve vision by absorbing stray light. Each day, the RPE supports photoreceptor renewal by phagocytosing shed photoreceptor outer segments and degrading them within lysosomes.

2011; Adijanto and Philp, 2014; Sonoda et al., 2009) and have emerged as a powerful system to study RPE function *in vitro*. However, they require at least four weeks on semi-permeable membrane supports to become fully differentiated (summarized in Table 1). Recent reports on establishing RPE monolayers from adult human eyes suggest a similar timeline to differentiation (Blenkinsop et al., 2013). This presents a challenge for live imaging studies that use exogenous expression of fluorescently tagged proteins because transgene expression does not last beyond 4–7 days, depending on the promoter used.

A number of recent studies have used RPE isolated from porcine eyes as *in vitro* models to address questions of trans-epithelial transport, outer segment phagocytosis, regulation of VEGF secretion and inflammation (Ablonczy and Crosson, 2007; Chew et al., 1993; Dintelmann et al., 1999; Dithmer et al., 2014; Hamann et al., 2003; Hammer et al., 2006; Joffre et al., 2007; Klettner et al., 2013; Miura et al., 2010; Muller et al., 2014; Shirasawa et al., 2013; Terasaki et al., 2013). Many of these studies used non-polarized porcine RPE cultures. A few (Miura et al., 2010; Shirasawa et al., 2013; Terasaki et al., 2013) used protocols that produced polarized RPE monolayers after 14–21 days in culture (summarized in Table 2), suggesting that porcine RPE could be an alternative *in vitro* model for use in live cell imaging if these monolayers could be induced to polarize within 7–10 days. Here, we demonstrate a culture method for porcine RPE with a short time to differentiation and establish the utility of these cultures for live imaging.

We present a simple, easily reproducible 3-step protocol to follow intracellular traffic in the RPE in real time: step 1 – establish and characterize primary RPE monolayers that become polarized within 7 days after plating on Transwell® filters; step 2 – transfect with genes of interest; and step 3 – perform high-speed live imaging. The salient features of this study are: (i) the culture protocol is straightforward and does not require specially formulated media,

Table 1
Comparison between polarized porcine adult, human fetal and human adult RPE.

Cell source	Porcine eyes (data from this study)	Human fetal	Human adult
Availability	Unlimited	Limited	Limited
Recommended growth medium	DMEM with 1% FBS and antibiotics; no other extracts, hormones or growth factors.	CEM replacement medium (Hu and Bok, 2001); MEM α with N1 supplement and THT (Maminishkis et al., 2006; Sonoda et al., 2009).	DMEM-F12 with N1 supplement, growth factors, hormones, etc (Blenkinsop et al., 2013).
Minimum time on filters for differentiation	7–14 days (Figs. 3–5)	~One month or more (Hu and Bok, 2001; Maminishkis et al., 2006; Sonoda et al., 2009)	~One month (Blenkinsop et al., 2013).
TER at one week (Ω cm^2)	~200 Ω cm^2 (Fig. 6)	~30–40 Ω cm^2 (Ablonczy et al., 2011)	~50–75 Ω cm (Blenkinsop et al., 2013)
TER after 1–3 months (Ω cm^2)	~400 Ω cm^2 (Fig. 6)	~200 Ω cm^2 at one month; >500 Ω cm^2 after 3 months (Ablonczy et al., 2011; Hu and Bok, 2001; Sonoda et al., 2009)	100–300 Ω cm (Blenkinsop et al., 2013).
Phagocytosis	OS clearance by 5 h (Fig. 7)	23 h (Gordiyenko et al., 2010)	15 h (Kennedy et al., 1994)
Transgene expression for live imaging?	Nucleofection >40% efficiencies; expression for ≥8 days (Fig. 8)	Not reported	Not reported (Blenkinsop et al., 2013)

Table 2
Features of studies using porcine RPE for *in vitro* models.

Aim and reference	Culture conditions	Polarity features
A2E-induced damage (Hammer et al., 2006)	DMEM with 20% FCS on fibronectin-coated plates	ZO-1 expression after 21 days in culture.
VEGF and barrier function (Ablonczy and Crosson, 2007)	On Transwell filters in DMEM/F12/ Ham with 10% FBS	TER at day 14–20 Ω cm^2 Maximum TER at 6 weeks ~70 Ω cm^2
VEGF and barrier properties (Miura et al., 2010)	DMEM with 10% porcine serum	TER at day 7–300 Ω cm^2 At day 21, ZO-1 at tight junctions;
TNFα and barrier properties (Shirasawa et al., 2013)	100,000 cells/cm^2 on fibronectin-coated filters in α-MEM with 1% FBS	TER at day 7–100 Ω cm^2; day 30–220 Ω cm^2 At day 14, RPE65, apical MCT1, basal laminin, ZO-1 at tight junctions; basolateral VEGF secretion.
TNFα and VEGF secretion (Terasaki et al., 2013)	100,000 cells/cm^2 on fibronectin-coated filters in α-MEM with 2% FBS	TER at day 7–200 Ω cm^2 At day 14, apical MCT1, basal laminin, ZO-1 at tight junctions and RPE65 expression. Basolateral VEGF secretion.
Bestrophin and phagocytosis (Muller et al., 2014)	1×10^6 cells/ml in 96-well plate in α-MEM with N1 and 5% FCS for 48 h	Non-polarized cells; Bestrophin-1 and β-catenin on the lateral membrane.
Polarized trafficking in primary RPE (this study)	300,000 cells/cm^2 on collagen-coated filters in DMEM with 1% FBS	TER at day 7–200 Ω cm^2 At day 7, apical Na,K-ATPase, ZO-1 at tight junctions and at day 14, RPE65 expression.

extracts or hormones; (ii) these RPE cells form tight monolayers with high TER, express differentiation markers and localize key proteins to the correct membrane domains and efficiently clear phagocytosed outer segments; (iii) we describe two different gene delivery protocols for polarized RPE that result in transgene expression that lasts for more than 7 days; and (iv) we demonstrate methods for high-speed live imaging of polarized RPE to track organelle transport. From a practical standpoint, use of porcine tissue to harvest RPE is highly advantageous since porcine eyes are considerably more available than human eyes. Because RPE and OS can be efficiently harvested from the same eyes using our protocol, it is a significant savings in terms of both cost and time. Our gene delivery protocols are suitable for biosafety level 1 (BSL-1) facilities unlike adeno, adeno-associated or lentiviral vectors that need enhanced BSL-2 or BLS-3 facilities. The live imaging methodology described here can be easily used with any commercially available microscopy systems.

This 3-step protocol fills an important niche in the study of RPE cell biology because it describes a method to study intracellular events that occur on timescales of milliseconds (e.g., organelle fission/fusion, tubulovesicular transport) or over periods of minutes to hours (e.g., biosynthetic protein sorting, endocytic transport, tissue morphogenesis). The ease of RPE culture, transfection and live imaging will not only allow investigation of basic cellular functions in the RPE in real time, but also enable comparative studies of healthy and compromised RPE to identify early functional deficits that could promote retinal disease.

2. Materials and supplies

Adult pig eyes (ages from 8 months to 5 years and both genders) were obtained from the Hart & Vold Meat Market (Baraboo, WI). Dulbecco's modified Eagle's medium (DMEM) with 4.5 g/L glucose, L-glutamine and sodium pyruvate and RPMI 1640 were from GIBCO Life technologies (Grand Island, NY). Trypsin was from Lonza (Basel, CH), Hanks balanced salt solution (HBSS) without calcium and magnesium, HBSS with calcium and magnesium, HEPES, penicillin/streptomycin, non-essential amino acids (NEAA) and EDTA were from Corning (Manassas, VA). Fetal bovine serum (FBS) from GIBCO was used during RPE harvest and FBS from American Type Culture Collection (ATCC) was used for RPE culture. Povidone-iodine was from Ricca (Arlington, TX), saponin and ciprofloxacin were from Sigma (St. Louis, MO) and mouse collagen IV was from BD Biosciences. T25 flasks, 12 mm and 24 mm diameter 0.4 μm pore size Transwell® filters were from Corning, glass-bottom 35 mm dishes were from Mattek (Ashland, MA), STX3 chopstick electrode was from World Precision Instruments (Sarasota, FL), ultracentrifuge tubes were from Beckmann Coulter (Brea, CA), Amaxa Nucleofector was from Lonza, electroporation cuvettes were from BTX (Holliston, MA) and small volume closed bath imaging chambers were from Harvard Apparatus (Hamden, CT). Immunofluorescence reagents: paraformaldehyde, slides and coverslips were from Electron Microscopy Sciences (Hatfield, PA), bovine serum albumin (BSA) was from Rockland (Gilbertsville, PA), mouse monoclonal 6-11B-1 anti-acetylated tubulin from Sigma (T6793), rat anti-ZO-1 (Xu et al., 2012), mouse monoclonal anti-alpha 1 Na,K⁻ATPase (ab7671) and mouse anti-RPE65 (ab13826) were from Abcam (Cambridge, MA), rabbit anti-LAMP1 from Cell Signaling (9091, Danvers, MA) and mouse-monoclonal (4D2) anti-rhodopsin from Millipore (MABN15), CellLight baculovirus fusion constructs, LysoTracker Green, AlexaFluor secondary antibodies and NucBlue were from Life Technologies (Grand Island, NY), rhodamine-phalloidin was from Cytoskeleton (Denver, CO) and Vectashield was from Vector Labs (Burlingame, CA). Immunoblotting reagents: DC assay kit was from Bio-Rad (Hercules, CA), 4–12% NuPAGE® Bis-Tris Precast Gels and the iBlot dry transfer system were from Invitrogen (Carlsbad, CA), goat anti-actin was from Santa Cruz (SC-1616, Dallas, TX), horseradish peroxidase-conjugated anti-rabbit, anti-mouse, or anti-goat secondary antibodies were from Southern Biotech (Birmingham, AL) and the ECL substrate was from Thermo Scientific (Rockford, IL).

3. Detailed methods

3.1. Porcine tissue handling and RPE harvest

Upon receipt, eyes were trimmed of excess tissue (Fig. 2A, B) and placed in 0.2% povidone-iodine (1% povidone-iodine diluted 1:5 in sterile distilled water) for 10 min on ice. Eyes were rinsed 5 times with sterile distilled water and placed in 1000 U/mL Penicillin-Streptomycin (10,000 U/mL diluted 1:10 in sterile distilled water) on ice for a minimum of 5 min. Anterior segments (including the entire lens and vitreous) were removed with a scalpel at the ora serrate (Movie 1). Eyecups (posterior poles) were placed into individual wells of 12-well tissue culture cluster plates. Eyecups were filled with 2 mL of PBS with 1 mM EDTA (pre-warmed to 37 °C) and incubated in a 37 °C 5% CO_2 incubator for 30 min (Fig. 2C). Incubation with EDTA loosens the neural retina from the RPE sheet. The retina was gently pulled and gathered at the center of the eyecup and clipped at the optic nerve head (Movie 2). Neural retinae were

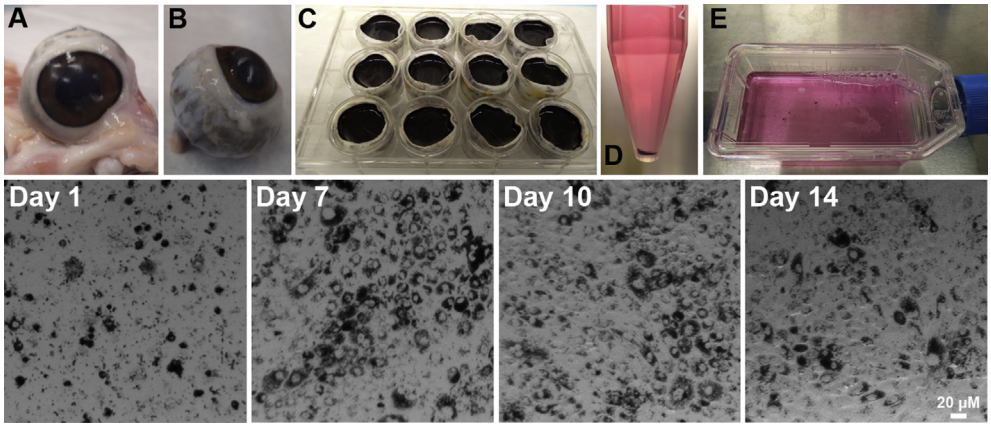

Fig. 2. Isolation of primary RPE from porcine eyes Top row: A, Freshly enucleated porcine eyes upon delivery. B, Eyes trimmed of excess tissue. C, Eyecups after removal of anterior segments, neural retina intact, filled with PBS-EDTA. D, RPE cells (pigmented pellet) collected after trypsinization. E, Cell suspension plated on T-25 flasks. Bottom row: Light micrographs of RPE cells harvested in Fig. 2 at 1, 7, 10 and 14 days after plating. Cells were grown in medium containing 10% FBS until day 7 and then switched to medium containing 1% FBS. Scale bar = 20 μm. See Methods for details.

collected and pooled for OS harvest as described below. Eyecups were placed into new sterile 12-well cluster plates and filled with 1 mL of pre-warmed 0.5% trypsin with 5.3 mM EDTA in HBSS without calcium and magnesium and incubated in a 37 °C 5% CO_2 incubator for 30 min. RPE cells were gently detached by repeated pipetting with a 10 mL serological pipet. The resulting RPE cell suspension (~2 mL) from two eyecups was combined and transferred to a 15 mL conical tube containing 8 mL of pre-warmed 10% FBS in 1× DMEM with 4.5 g/L glucose, L-glutamine and sodium pyruvate to inactivate the trypsin (Movie 3). Eyecups were rinsed out with 1 mL each of pre-warmed trypsin to harvest any remaining RPE and added to the conical tubes (total of 12 mL–8 mL FBS plus 4 mL trypsin cell suspension). This was repeated for all eyecups. Tubes were centrifuged (Eppendorf, model 5702, Hauppauge, NY) for 4 min at 300 RCF and the supernatant was aspirated (Fig. 2D). Cell pellets from five tubes (RPE from 10 eyecups) were pooled and resuspended in 14 mL of 10% ATCC FBS in 1× DMEM with 4.5 g/L glucose, L-glutamine and sodium pyruvate, 1% NEAA and 1% penicillin/streptomycin. 7 mL of this suspension was plated onto one T25 flask and distributed over the surface of the flask by gentle shaking (Fig. 2E). Flasks were kept at 37 °C in a 5% CO_2 incubator.

Supplementary video related to this article can be found at http://dx.doi.org/10.1016/j.exer.2014.05.003.

Porcine RPE plated on T-25 flasks reached confluence within 7 days (Fig. 2, bottom row). Cell monolayers were pigmented and showed the characteristic cobblestone morphology. For the first week the cells were grown in 7 mL 10% ATCC FBS in 1× DMEM with 4.5 g/L glucose, L-glutamine and sodium pyruvate, 1% NEAA and 1% PenStrep. Cells were fed with fresh growth medium at day 3 after harvest. At day 7, cells were switched to medium containing 1% FBS (ATCC) in 1× DMEM (DMEM with 4.5 g/L glucose, L-glutamine and sodium pyruvate), 1% NEAA, 1% PenStrep, and 10 μg/mL ciprofloxacin. Decreasing serum concentration to 1% is necessary for the cells to stop proliferating and undergo differentiation. Studies in rat RPE have shown that high serum in the medium prevents expression of tight junction proteins (Chang et al., 1997a, 1997b). It is also essential to grow the cells in 1% serum prior to plating them on filters because culture conditions influence gene expression profiles (Tian et al., 2005).

3.2. Establishment of polarized monolayers

Two weeks after culture, growth medium was aspirated and RPE on T25 flasks were washed HBSS without calcium or magnesium and incubated with fresh HBSS without calcium or magnesium for 15 min at 37 °C in a 5% CO_2 incubator. The HBSS was aspirated and replaced with 3 mL 0.25% trypsin with 2.21 mM EDTA and the flasks were returned to the incubator for 6 min. Trypsin was neutralized with 6 mL 1% FBS growth media and the suspension was collected in 15 mL conical tubes. Cells were centrifuged for 4 min at 300 RCF, supernatant aspirated and cell pellets resuspended in fresh 1% FBS growth medium.

RPE were plated at confluence onto semi-permeable polyester Transwell® filters, 0.4 μm pore size. Filters were first coated with 5 μg/cm^2 mouse collagen IV for one hour room temperature and washed twice with HBSS without Ca^{2+} or Mg^{2+}. Cells were typically plated at a density of 300,000 cells per cm^2 on either 12 mm or 24 mm filters, depending on the experimental paradigm. Filters were maintained in a 37 °C and 5% CO_2 incubator for 2–4 weeks and fed fresh 1% FBS growth medium every 3–4 days. 12 mm filters were fed 0.3 mL media in the top chamber and 0.7 mL media in the bottom chamber and 24 mm filters were fed 1 mL in the top chamber and 1.5 mL media in the bottom chamber.

Since published reports indicate that it takes ≥four weeks for human RPE cultures (Blenkinsop et al., 2013; Geisen et al., 2006; Hu and Bok, 2001; Maminishkis et al., 2006; Sonoda et al., 2009) and ≥14 days for porcine RPE cultures (Shirasawa et al., 2013; Terasaki et al., 2013) to become polarized on filters (see Tables 1 and 2), we first checked the expression of polarity markers in our RPE cultures after two weeks on filters. Immunostaining showed that, as early as two weeks, these cells form densely packed, pigmented monolayers that localize ZO-1 to the tight junctions and acetylated tubulin to the primary cilium (Nishiyama et al., 2002) (Fig. 3). These data indicate that plating at confluence in low FBS medium is critical for adult primary porcine RPE to form polarized monolayers within 7 days.

3.3. Relationship between plating density and development of polarity in RPE monolayers

Studies have shown that the expression of RPE-specific differentiation markers such as RPE65 is abundant in freshly harvested native RPE but is lost within two weeks of culture when cells are plated at low density and allowed to proliferate to reach confluence over 4–8 weeks (Hamel et al., 1993). Moreover, RPE cells plated at low confluence have immature intercellular junctions, low packing density and express high levels of proliferation markers like Ki-67 (Kaida et al., 2000). A recent report suggests that plating density could influence time to polarity for human fetal RPE, based on

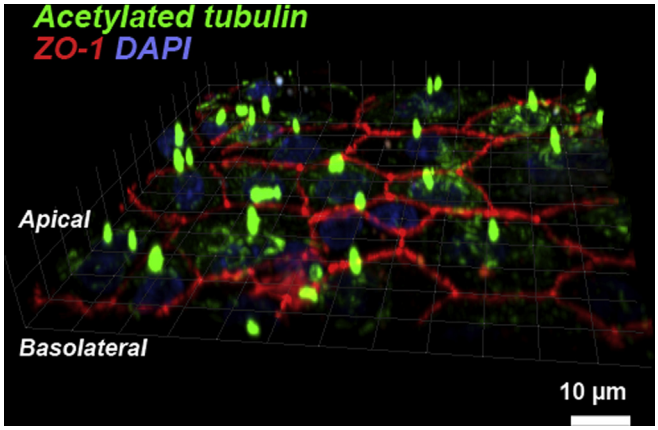

Fig. 3. Immunostaining of polarized RPE monolayers RPE cells grown on Transwell® filters for two weeks were fixed and labeled with antibodies to acetylated tubulin (green) and the tight junction protein ZO-1 (red). Nuclei are stained with DAPI (blue). The image shows an x–z scan of the RPE cell sheet with the primary cilia (stained for acetylated tubulin) and the organization of the tight junction network between cells can be clearly discerned. Scale bar = 10 μm.

qualitative assessment of RPE morphology and packing density (Adijanto and Philp, 2014). We hypothesized that RPE65 gene expression would be retained in primary RPE plated at confluence because they would not undergo de-differentiation or proliferation, unlike sparsely plated cells. We tested this by plating cells at three different densities on Transwell® filters: 50,000, 150,000 or 300,000 cells/cm^2. At 7, 14 and 21 days on Transwell® filters, transepithelial electrical resistances (TER) were measured and cells were fixed in 2% paraformaldehyde for 10 min at room temperature and immunostained for polarity markers (see below).

3.4. Immunofluorescence staining and imaging to determine polarity

Cells grown on Transwell® filters were fixed in 2% paraformaldehyde (PFA) in PBS. Membranes were excised from the filters and blocked in 1% BSA in PBS containing 1 mM calcium chloride and 1 mM magnesium chloride for 30 min. Cells were incubated with primary antibodies for 1 h at room temperature. Primary antibodies were diluted in blocking buffer with 0.1% saponin and used as follows: mouse monoclonal 6-11B-1 anti-acetylated tubulin 1:1000, rat anti-Z0-1 1:3000, mouse monoclonal anti-alpha 1 Na,K$^-$ATPase 1:200, mouse anti-RPE65 1:200, rabbit anti-LAMP1 1:100 and mouse-monoclonal (4D2) anti-rhodopsin 1:500. Cells were washed thrice, 5 min each with blocking buffer to remove unbound antibodies and incubated for 30 min at room temperature with anti-mouse or anti-rabbit AlexaFluor 488 secondary antibodies diluted in blocking buffer at 1:500, rhodamine-phalloidin at 1:200, and 2 drops of NucBlue per mL of antibody solution. Filters were washed thrice, 5 min each with blocking buffer and a final 5-min wash in PBS with calcium and magnesium. Filters were mounted on clean slides under coverslips with Vectashield and sealed with clear nail enamel. Cells were

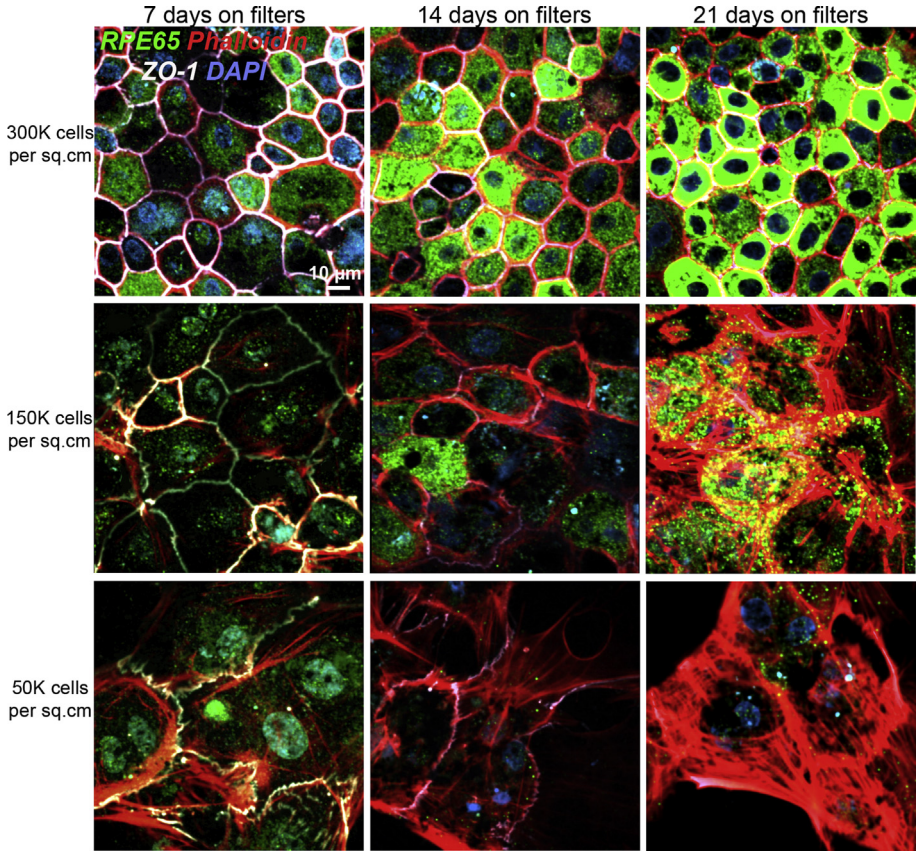

Fig. 4. Expression of RPE65 in porcine RPE cultures depends on initial plating density Immunofluorescence images of primary porcine RPE plated on Transwell® filters at three different plating densities: top row, 300,000 cells/cm^2; middle row: 150,000 cells/cm^2 and bottom row: 50,000 cells/cm^2, and cultured for 7 days (first column), 14 days (middle column) or 21 days (third column). At each time point, cells were fixed and stained with antibodies to RPE65 (green) and ZO-1 (white) and stained with phalloidin to label the actin cytoskeleton and DAPI to label nuclei. Cells plated at low densities appear larger because they are flatter and fibroblastic compared to cells plated at confluence, which are taller, epithelial and compactly packed. Scale bar = 10 μm.

imaged with the Andor Revolution XD spinning disk confocal microscope (see below) at 100 ms exposure using a 60x 1.4 NA oil objective.

As shown in Fig. 4, RPE65 protein expression could be robustly detected in cultures that were plated at confluence, i.e., at 300,000 cells/cm^2. Cells plated at 50% or lower confluence had low RPE65 expression. Notably, under sub-confluent conditions, tight junctions labeled by ZO-1 became discontinuous and distorted. Localization of ZO-1 to the tight junctions is modulated by cell–cell contacts in Madin-Darby canine kidney (MDCK) cells (Siliciano and Goodenough, 1988) and this also applies to primary RPE. Phalloidin staining showed that the actin cytoskeleton was disorganized in cells plated at low densities with many actin stress fibers clearly visible. RPE cell morphologies were also strikingly altered in cells plated at low densities and we observed cells that were more fibroblastic (flat, large cells) rather than epithelial (tall, compact cells) (Fig. 4).

Next, we examined the expression and localization of Na^+,K^+-ATPase in the RPE as a function of plating density and days in culture. *In situ*, Na^+,K^+-ATPase is present on the RPE apical membrane and pumps Na^+ out of and K^+ into the RPE cell. This helps maintain a high Na + environment in the sub-retinal space, which is necessary for photoreceptor dark current and photo-transduction (Ames et al., 1992; Quinn and Miller, 1992). In RPE cultures from chicken embryos, Na^+,K^+-ATPase becomes nonpolar upon culture (Rizzolo, 1990), whereas human fetal RPE monolayers polarize Na^+,K^+-ATPase apically only after 4 weeks on Transwell® filters (Geisen et al., 2006; Hu and Bok, 2001; Maminishkis et al., 2006; Sonoda et al., 2009). Immunofluorescence images showed that in our primary porcine RPE monolayers, Na^+,K^+-ATPase was localized apically as early as 7 days post-plating in cells seeded at confluence (Fig. 5). When cells were plated at low densities, Na^+,K^+-ATPase was found at the apical membrane only after 3 weeks on Transwell® filters.

3.5. Trans-epithelial electrical resistance (TER) measurements

Tight junctions between adjacent RPE cells prevent transport of solutes via the paracellular route and help the RPE regulate movement of solutes and metabolites into and out of the retina. Resistance to passive diffusion of ions across the monolayer is a measure of the barrier function or "tightness" of the epithelial cell sheet (Madara, 1998). TER across isolated preparations of fresh fetal and adult human RPE were reported to be in the range of

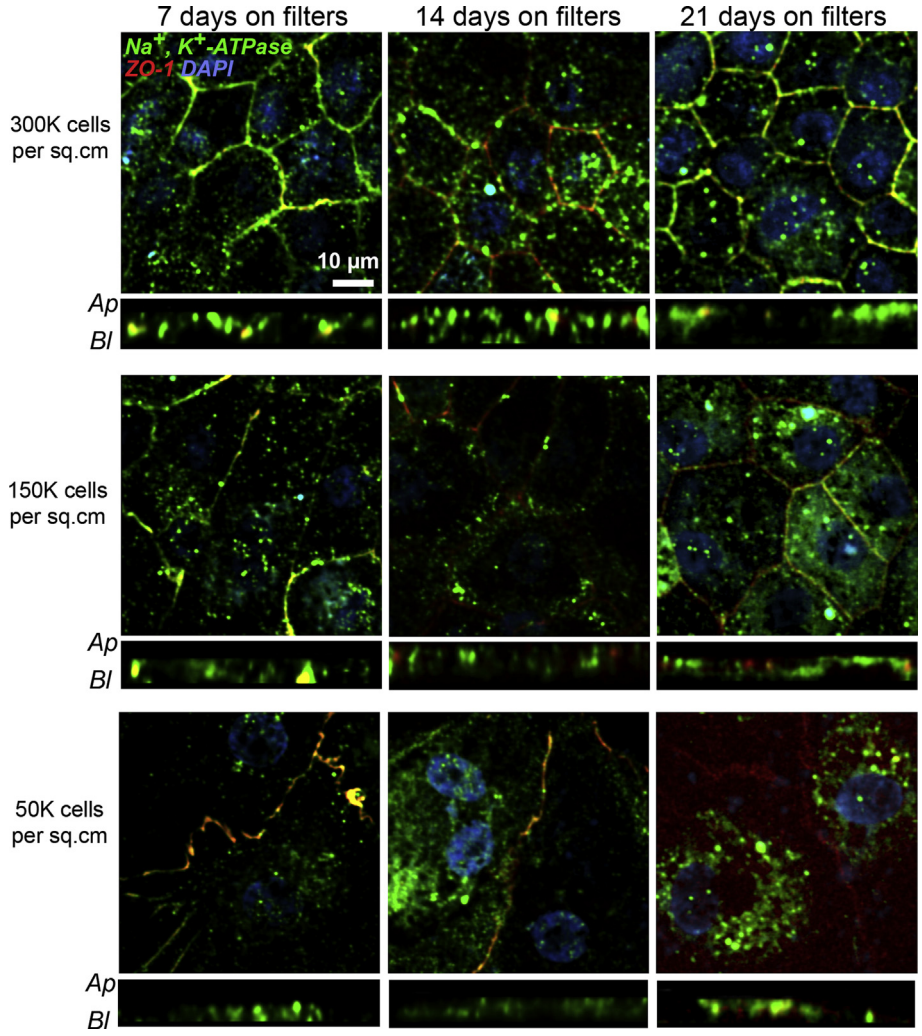

Fig. 5. Polarity of Na+, K+-ATPase in porcine RPE cultures Immunofluorescence images of primary porcine RPE plated on Transwell® filters at three different plating densities: top row, 300,000 cells/cm^2; middle row: 150,000 cells/cm^2 and bottom row: 50,000 cells/cm^2, and cultured for 7 days (first column), 14 days (middle column) or 21 days (third column). At each time point, cells were fixed and stained with antibodies to Na^+, K^+-ATPase (green) and ZO-1 (red). Nuclei stained with DAPI are in blue. Both *en face* and x-z views are shown. Ap – apical; Bl – basolateral. Scale bar = 10 µm.

206 ± 151 Ω cm^2 (Quinn and Miller, 1992). Published data show that primary human fetal RPE attain TER values of 100 Ω cm^2 or more only after at least 30 days in culture (Hu and Bok, 2001; Maminishkis et al., 2006; Sonoda et al., 2009). For porcine RPE, plating at 100,000 cells/cm^2 on Transwells resulted in TER of 150–200 Ω cm^2 after 7–14 days on filters (Shirasawa et al., 2013; Terasaki et al., 2013).

We measured TER of RPE monolayers on Transwell® filters with the STX3 chopstick electrode weekly for 3 consecutive weeks. Transwell® filters were filled with pre-warmed media and TER readings were obtained after placing the electrodes according to the manufacturer's instruction. TER measurements of collagen-coated filters without cells were used for background subtraction. Resistance per unit area was calculated by multiplying background-subtracted TER values by the area of the Transwell® filter membranes.

Our primary porcine RPE cultures exhibited a TER of 203 ± 10 Ω cm^2 as early as 7 days in culture when plated at 300,000 cells/cm^2, which increased to 398 ± 19 Ω cm^2 after 14 days (Fig. 6). In agreement with the immunostaining data shown in Figs. 6 and 7, TER values of cells plated at low densities were low and did not cross 100 Ω cm^2 even after 21 days in culture (Fig. 6). Collectively, these data suggest that when primary porcine RPE are plated at confluence on collagen-coated Transwell® filters, they form tight monolayers with relatively high TERs and express RPE differentiation markers within 7–14 days in culture.

3.6. Photoreceptor outer segment phagocytosis and clearance

A major function of the RPE *in vivo* is the daily phagocytosis and clearance of shed photoreceptor outer segment disks (Kevany and Palczewski, 2010). Efficient lysosomal clearance of phagocytosed disks is critical for preventing accumulation of cellular debris within the RPE, which can contribute to RPE dysfunction and retinal disease (Lakkaraju, 2012). A significant limitation of currently available RPE cell lines is that it takes ≥24 h for these cells to completely clear ingested outer segments (Diemer et al., 2008; Finnemann et al., 2002; Lakkaraju et al., 2007). Studies on rodent RPE suggest that outer segment disk clearance occurs fairly rapidly, within 2–10 h after phagocytosis depending on the experimental paradigm (Gibbs et al., 2003; Nandrot et al., 2004). Limited data are available on the kinetics of outer segment clearance in human and porcine primary RPE cultures: one study on human fetal RPE (Gordiyenko et al., 2010) and another on adult RPE (Kennedy et al., 1994) showed that these cells take 15–23 h to clear phagocytosed outer segments.

To determine the efficiency of outer segment engulfment and digestion by our porcine primary RPE cultures, we isolated rod outer segments from porcine eyecups at the same time as RPE harvest, fed them to polarized porcine RPE monolayers and followed phagocytosis and degradation by immunofluorescence and immunoblotting as detailed below.

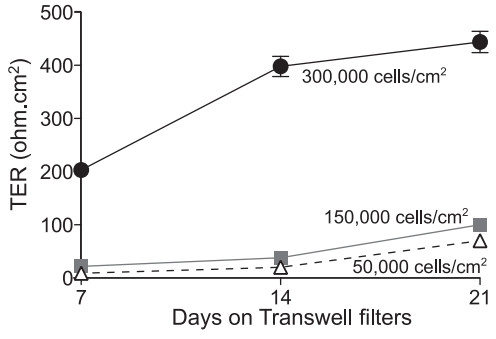

Fig. 6. Trans-epithelial electrical resistances (TER) of primary porcine RPE monolayers. TER measurements of cells in Transwell®s plated at three different densities: 300,000 cells/cm^2 (black circles); 150,000 cells/cm^2 (gray squares) or 50,000 cells/cm^2 (open triangles). Values plotted are Mean ± S.E.M., three replicates per data point.

3.6.1. Outer segment isolation

Outer segments were purified from porcine eyes using modifications of previously published protocols for bovine eyes (Finnemann et al., 1997; Molday et al., 1987). Under dim light, ~20 retinae from porcine eyes were collected into a conical tube (covered with foil) containing 7.5 mL ice-cold homogenization solution (20% sucrose, 20 mM tris acetate pH7.2, 2 mM $MgCl_2$, 10 mM glucose, 5 mM taurine). The tube was then shaken with moderate force for 2 min and the resulting homogenate was filtered through cotton gauze three times successively to remove tissue fragments. The filtrate was transferred on top of a continuous sucrose gradient and centrifuged for 1 h at 25,400 rpm (84,000 rcf) at 4 °C (Thermo Scientific Sorvall WX Ultra Series ultracentrifuge). The continuous sucrose gradient was generated in ultracentrifuge tubes 2 h prior to outer segment isolation using a gradient maker with 60% and 25% sucrose solutions, both supplemented with 20 mM Tris-acetate pH7.2, 10 mM glucose, and 5 mM taurine. After centrifugation, a single pale orange-pink band was observed near the upper third of the gradient. This band was carefully collected with a pipette into a conical tube and diluted with 5 volumes of wash solution 1 (20 mM Tris acetate pH 7.2, 5 mM taurine) and centrifuged at 3000 RCF at 4 °C for 10 min. Wash solution 1 was aspirated and the resulting bright orange pellet was resuspended in wash solution 2 (10% sucrose, 20 mM Tris acetate pH 7.2, 5 mM taurine) and centrifuged at 3000 RCF at 4 °C for 10 min. After aspiration of wash solution 2, the pellet was resuspended in wash solution 3 (10% sucrose, 20 mM sodium phosphate pH 7.2, 5 mM taurine) and centrifuged again. The final pellet was resuspended in 1× DMEM supplemented with 2.5% sucrose and counted using a hemocytometer to check the yield. The outer segment suspension was aliquoted for storage at −80 °C.

3.6.2. Outer segment phagocytosis assays

Outer segments were thawed, centrifuged at 2600 RCF for 5 min and the supernatant aspirated. The outer segment pellet was resuspended in 1× DMEM supplemented with 1% NEAA and 1% FBS (ATCC). Porcine RPE cells on filters were incubated with outer segments (~10 OS/cell) for 2 h at 37 °C. One set of cells were either fixed for immunofluorescence or harvested for immunoblotting (0 time point). From the remaining filters, outer segments were washed out and cells were fed with fresh 1% FBS-containing growth medium and incubated for an additional 1, 3 or 5 h and then fixed or harvested to follow OS clearance kinetics (Fig. 7A). Immunostaining showed that after two hours, rhodopsin-labeled outer segment particles were in lysosomes labeled with lysosome-associated membrane protein 1 (LAMP1). Rhodopsin signal gradually decreased 3 and 5 h after outer segment phagocytosis, indicative of rhodopsin degradation (Fig. 7B). For immunoblotting, cells were harvested by trypsinization and lysed in HNTG buffer (50 mM Hepes, 150 mM NaCl, 10% glycerol, 1.5 mM $MgCl_2$, 1% TX-100) supplemented with protease inhibitors. Protein concentrations were measured using the DC assay. Samples (20 μg) were run in 4–12% NuPAGE® Bis-Tris precast gels at 200 V. Proteins were transferred onto nitrocellulose membranes using iBlot dry transfer system, blocked in 5% milk in Tris-buffered saline with 0.1% Tween-20 (TBS-T) for 1 h before incubating in primary antibody overnight at 4 °C. Primary antibodies used were: mouse-monoclonal (4D2) anti-rhodopsin 1:750 and goat anti-actin 1:500. After three 5-min washes in TBS-T, membranes were incubated in 1:10,000 horseradish peroxidase-conjugated anti-rabbit, anti-mouse, or anti-goat secondary antibodies for 45 min. Membranes were then

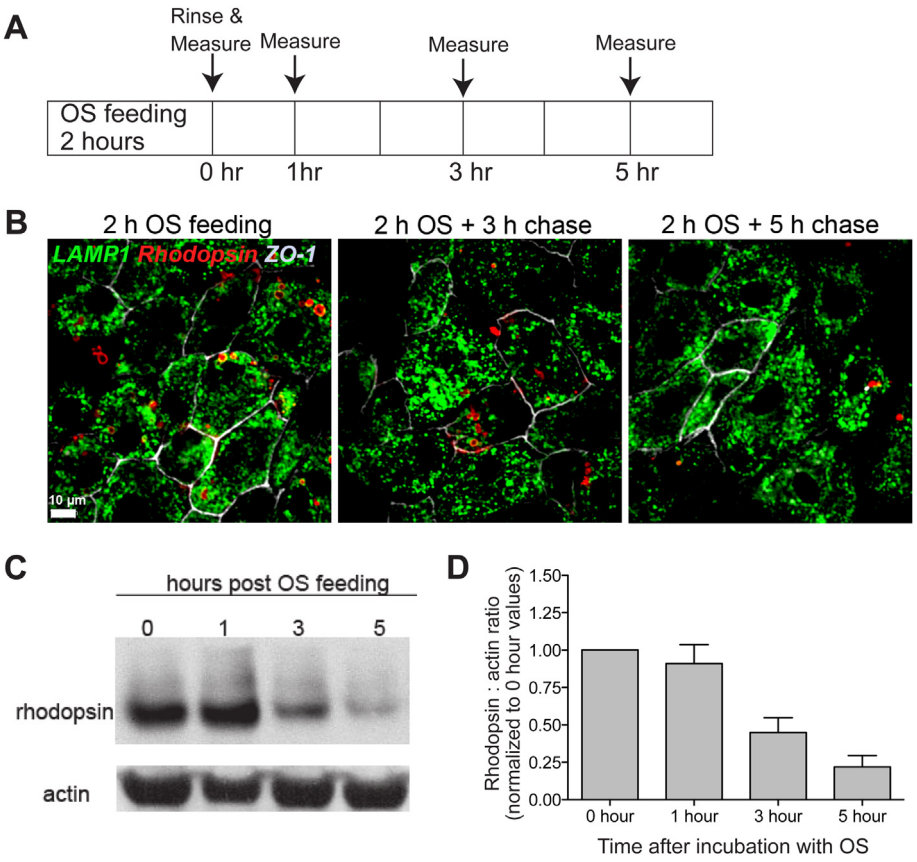

Fig. 7. Phagocytosis and clearance of photoreceptor outer segments by primary porcine RPE cultures. A, Experimental design. Cells were fed outer segments (OS) for 2 h, rinsed and harvested for analysis or incubated in fresh medium for an additional 1, 3 or 5 h. B, Immunofluorescence images of OS-fed cells labeled with antibodies to LAMP1 (green) to label lysosomes, rhodopsin (red) to follow the fate of phagocytosed OS and ZO-1 (gray–white). Scale bar: 10 μm. C, Representative immunoblot showing rhodopsin degradation with time by primary porcine RPE monolayers. Loading control: actin. D, Quantification of rhodopsin:actin levels in C relative to the 0 time control. Mean ± S.E.M of three independent experiments.

washed thrice for 15 min each before signal detection using ECL substrate. Our data showed that majority of the rhodopsin is cleared from our primary RPE cultures with 5 h after outer segment phagocytosis (Fig. 7C). Thus, polarized porcine RPE monolayers retain functional characteristics of native RPE and ingest and clear photoreceptor outer segments with high efficiency.

3.7. Expression of transgenes in primary porcine RPE

Live imaging of polarized RPE monolayers expressing fluorescently tagged proteins of interest is a powerful technique to investigate basic questions of RPE morphogenesis, intracellular trafficking and polarized sorting and for identifying early cellular dysfunction that could contribute to disease. A significant limitation of the ≥14 day culture times required for differentiation of human and porcine primary RPE monolayers is that once polarized, these cells are not easily amenable to transfection for expressing fluorescently tagged proteins. We present two different protocols for expressing transgenes in RPE cells.

Protocol 1. Transfection of cells in suspension prior to plating on filters: Cells on T25 flasks were harvested by trypsinization and ~1.5 million RPE were suspended in 100 μL of Amaxa nucleofection buffers (kit L) along with 5 μg of appropriate plasmid. The cell suspension was transferred to an electroporation cuvette and placed in the Amaxa Nucleofector II device. Cells were nucleofected using the L-005 program on the instrument. The transfected cell suspension was transferred to a microfuge tube containing 600 μL pre-warmed RPMI 1640 medium (Mediatech) and incubated at 37 °C for at least 10 min before plating onto Transwell® filters or serum-coated glass-bottom dishes (Mattek, Ashland, MA) or collagen-coated Transwell® filters for live imaging. Nucleofection resulted in transfection efficiencies of ~40% or higher, depending on the size of plasmid. After plating on filters or glass-bottom Mattek dishes, cells expressed the exogenous plasmid driven by the cytomegalovirus promoter (CMV) for up to 8 days (Fig. 8A).

Protocol 2. Baculovirus transduction of polarized monolayers: Cells on filters were incubated with CellLight® BacMam 2.0 baculovirus insect expression system to efficiently transduce cells according to the manufacturer's instructions. The recommended amount of CellLight particles to cell numbers is 10–50 particles/cell and needs to be optimized for each fusion protein. We used ~5 × 10^6 particles for a 12 mm Transwell filter with ~300,000 cells (roughly 17 particles per cell). Cells were incubated with the CellLight particles overnight and imaged the next day.

3.8. Spinning disk confocal microscopy for live imaging and 4-D image analysis

Cells were imaged 48–96 h after transfection using the Andor Revolution XD microscope system equipped with a Yokogawa CSU-X1 confocal spinning disk head, a Nikon Eclipse Ti inverted microscope with a 100× Apo TIRF objective (compatible with both confocal and TIRF microscopy) and an ASI motorized stage with piezo Z for rapid Z-stack acquisition, an Andor laser combiner with four solid state lasers at 405, 488, 561, and 640 nm and corresponding band-pass filter sets, an iXon x3 897 EM-CCD camera (for

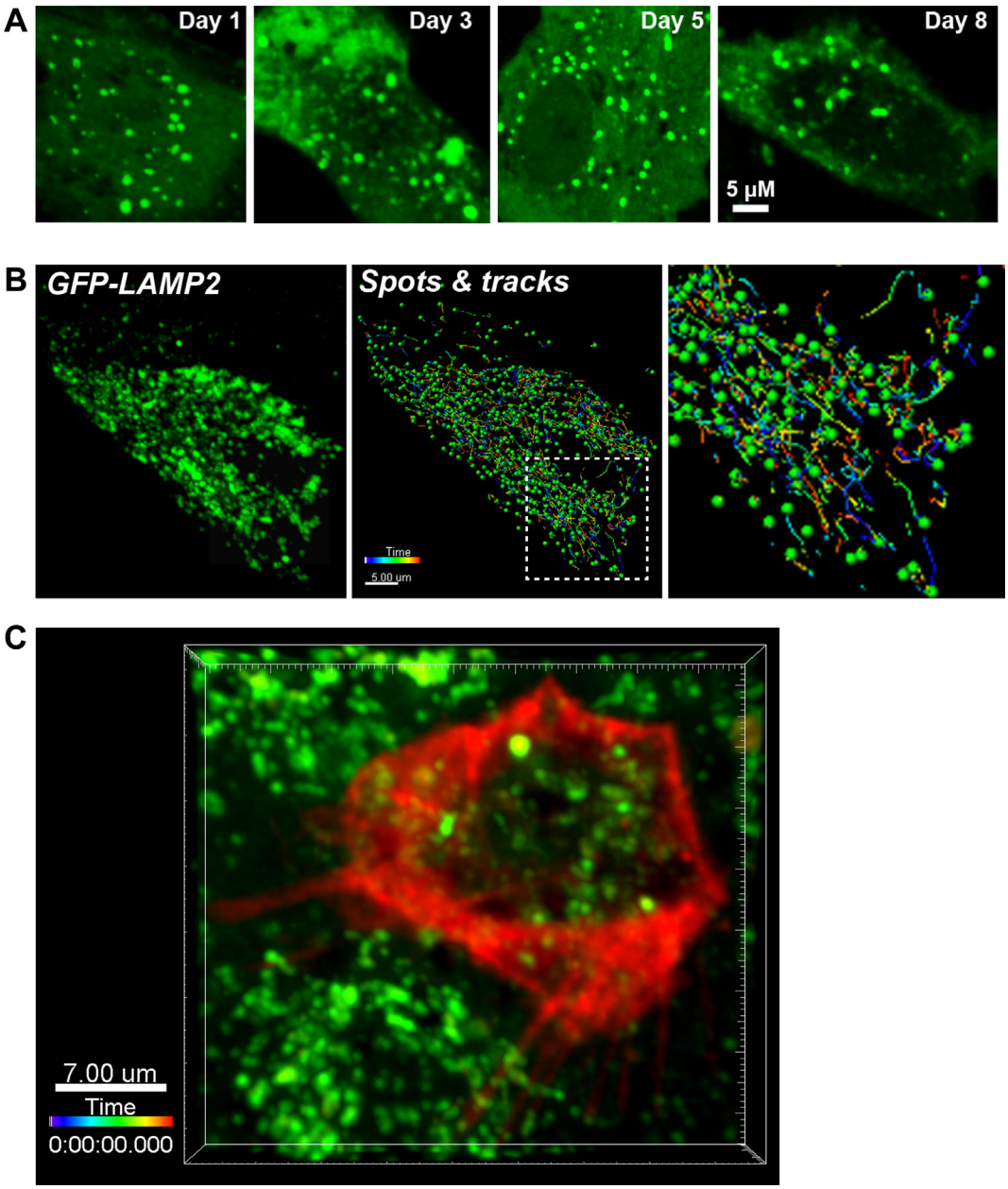

Fig. 8. Transfection and live imaging of organelle traffic in primary porcine RPE. A, Time course of EGFP-LC3 expression after nucleofection. A single cell is shown in high magnification. B, Left panel: Still image from a spinning disk confocal movie of a single RPE cell expressing the lysosomal marker EGFP-LAMP2. Middle panel: Spots and tracks analysis of the cell to follow the trajectories of individual lysosomes. Right panel: magnified view of boxed area in the middle panel. Scale bar: 5 μm. Time stamp shows the lifetime of individual tracks. C, Still image from multicolor live imaging of primary RPE expressing CellLight® actin-RFP (red) and labeled with LysoTracker® green.

confocal microscopy) and a Neo sCMOS camera (for TIRF microscopy). IQ2 software (Andor) was used for image acquisition and Imaris x64 software (Bitplane, Zurich, CH) for image analysis. Cells on filters were excised using a scalpel blade and mounted face down (apical side down) in a small-volume closed bath chamber suspended in a drop of imaging medium (HBSS with calcium and magnesium, 20 mM HEPES and 4.5 g/L glucose) between two coverslips. For cells grown on glass-bottom Mattek dishes, growth medium was replaced with imaging medium immediately before microscopy. For transfected RPE cells, 2–10 min worth of rapid z-stacks were acquired with this system. Trafficking data was collected from 3 to 6 separate transfections and at least 30 movies were captured for each transfection and treatment. During image acquisition care was taken to maintain the same laser power, exposure and electron-multiplying gain settings.

Image analysis of these data was performed using the Spots and Tracks modules of Imaris x64 (Bitplane) software to determine parameters such as track displacement, mean speed, track duration etc. and provide a real-time measure of organelle trafficking in the RPE. Similar analyses can be performed using other commercially available software such as Metamorph (Molecular Devices), Volocity (PerkinElmer) or Axiovision (Zeiss).

Cells expressing EGFP-tagged LAMP2 (lysosome-associated membrane protein 2) were imaged live using spinning disk confocal microscopy using the 488 laser line (Movie 4). Analysis of real-time tubulovesicular trafficking using the Spots and Tracks modules of Imaris software (Fig. 8B) showed that ~50% of LAMP2-labeled organelles move with speeds $\geq$0.5 μm/s. For multicolor imaging, polarized cells on Transwell filters expressing CellLight Actin-RFP were incubated with LysoTracker Green to label

lysosomes. The filters were excised and placed in a small volume closed volume chamber and imaged using the 488 and 561 laser lines (Fig. 8C and Movie 5).

Supplementary video related to this article can be found at http://dx.doi.org/10.1016/j.exer.2014.05.003.

4. Potential pitfalls and troubleshooting

4.1. Inter-experiment variability due to pooling cells from different eyes

Our protocol pools cells from different eyes and the flasks are a heterogeneous mix of different ages/sexes/health statuses as opposed to a single source of cells (as in the case of human fetal RPE), which could introduce some inter-experimental variability. In our experience, this is not a significant issue if data are collected from triplicates from at least three independent platings. Alternatively, close communication with vendors to acquire eyes only from animals of matched age, gender, etc. could also help circumvent this potential problem.

4.2. Maintaining continuous supply of primary RPE

We have had limited success in recovering cells from frozen stocks and these cells do not divide significantly in culture. This prevents passaging of the cells beyond P1 (i.e., plating on Transwell® filters). Moreover, cells passaged beyond this lose pigment and become fibroblastic. To maintain a continuous supply of cells, we isolate RPE cells every week so we don't have to depend upon frozen stocks.

4.3. Problems with generating healthy polarized monolayers of porcine RPE

We have observed that primary RPE are healthiest when grown in medium containing FBS from ATCC rather than in medium with FBS from other vendors. Because pigs are natural carriers of several mycoplasma strains (Drexler and Uphoff, 2002), we grow cells with ciprofloxacin as a prophylactic to prevent mycoplasma contamination of our cultures. In our experience, RPE do not polarize well on filters with diameters less than 10–12 mm and cells seem to form better monolayers on collagen-coated polystyrene filters compared to laminin-coated polystyrene or polycarbonate filters.

4.4. Problems with transgene expression

For Amaxa nucleofection, highest transfection efficiencies are obtained with cells that are no more than 2–3 weeks old after initial harvest from porcine eyes. Older cells yield poor transfection efficiencies. We typically use ~5 μg DNA (for plasmids with a cytomegalovirus promoter) and 1.5 million cells per transfection. This can be optimized depending on the promoter and plasmid size. However, plasmids with a total size (fluorescent reporter + gene of interest) greater than 5 kilobases are poorly expressed after nucleofection. In such cases, adenovirus vectors, which can accommodate inserts up to 7 kb are a likely alternative.

4.5. Issues with live imaging

Primary RPE cells have significant autofluorescence due to melanin granules that can make it difficult to detect transgene expression in cases of poor transfection efficiency or when the fluorescent tag has poor quantum efficiency. Untransfected control cells should be imaged for each experiment to set the threshold for background autofluorescence. Fluorescent reporters used for live imaging should ideally have the best combination of high quantum efficiency, brightness and photostability (Shaner et al., 2005).

4.6. Advantages and disadvantages of the pig as a model system to study RPE and retinal function

Pigs diverged from humans ~70 million years ago compared to mice, which diverged from humans around 91 million years ago (Groenen et al., 2012). There are several advantages of using porcine tissue including low cost, wide availability, short death-to-RPE harvest time and limited ethical concerns compared to those associated with human fetal tissue. For studying diseases that affect the central retina like AMD, pigs have unique advantages compared to mice because among non-primates, the pig eye is most similar to that of humans with a cone-rich area in a central horizontal band (the area centralis), which is analogous to the human macula (Sanchez et al., 2011). Recent studies show that the porcine immune system has many similarities to that of humans (Mair et al., 2014), which could be useful in modeling diseases like AMD that have a strong immune component (Ambati et al., 2013). Indeed, choroidal neovascularization or wet AMD has been modeled in pigs (Lassota et al., 2007) and transgenic porcine models of retinitis pigmentosa and autosomal-dominant form of Stargardt disease have also been developed (Petters et al., 1997; Ross et al., 2012; Sommer et al., 2011). These studies suggest that the pig could be a powerful model to study AMD and other complex retinal diseases.

Pigs reach sexual maturity around 6 months of age and have an average life span of 10–15 years. In our studies, we primarily used eyes from animals 8 months to 5 years of age, with the majority being fairly young, around 1 year old. This could be a limitation for studies comparing young and aged retinal tissue. On the other hand, the use of RPE from young pigs could enable mechanistic studies to identify early deficits in RPE function that could contribute to disease. Another potential disadvantage is that pigs do not express key proteins implicated in the pathogenesis of AMD such as ARMS2/HTRA1 or multiple apolipoprotein E (ApoE) isoforms. In this regard, although non-human primates express ARMS2 (Francis et al., 2008), they express only one ApoE isoform, unlike humans who have three ApoE alleles (Keene et al., 2011). Thus, although our porcine RPE model has significant advantages over currently available *in vitro* RPE model systems, it cannot conceivably replicate all features of human RPE and, depending on the experimental paradigm, comparative studies using human tissue will likely be necessary.

Since there is, as yet, no "gold standard" *in vitro* RPE model (Rizzolo, 2014), our primary porcine RPE model fulfills a key niche for RPE cell biologists. The detailed 3-step protocol presented here to culture, transfect and image polarized primary RPE monolayers is a powerful tool that can be used to study diverse processes (organelle biogenesis and trafficking, cellular energetics and clearance, cytoskeletal transport, etc.) within the RPE that will likely yield valuable insight into RPE function in health and disease.

Acknowledgments

We thank Ingrid Meschede (laboratory of Clare Futter, University College, London) and Dena Almeida (Weill Cornell Medical College, Cornell University) for sharing their protocols for culturing porcine and bovine RPE, respectively. Supported by NIH P30 EY016665, and grants from the Research to Prevent Blindness Foundation, American Federation for Aging Research, BrightFocus Foundation (M2009-093), Karl Kirchgessner Vision Research Foundation, Reeves Foundation for Macular Degeneration Research and gifts from the Schuette-Kraemer family for macular degeneration research. A.L. is the Retina Research Foundation Rebecca Meyer Brown Professor and the recipient of a career development award from the Research to Prevent Blindness Foundation.

References

Ablonczy, Z., Crosson, C.E., 2007. VEGF modulation of retinal pigment epithelium resistance. Exp. Eye Res. 85, 762–771.

Ablonczy, Z., Dahrouj, M., Tang, P.H., Liu, Y., Sambamurti, K., Marmorstein, A.D., Crosson, C.E., 2011. Human retinal pigment epithelium cells as functional models for the RPE in vivo. Investig. Ophthalmol. Vis. Sci. 52, 8614–8620.

Adijanto, J., Philp, N.J., 2014 Jan 28. Cultured primary human fetal retinal pigment epithelium (hfRPE) as a model for evaluating RPE metabolism. Exp. Eye Res. pii: S0014-4835(14)00030-X. http://dx.doi.org/10.1016/j.exer.2014.01.015. (Epub ahead of print) Review.

Ambati, J., Atkinson, J.P., Gelfand, B.D., 2013. Immunology of age-related macular degeneration. Nat. Rev. Immunol. 13, 438–451.

Ambati, J., Fowler, B.J., 2012. Mechanisms of age-related macular degeneration. Neuron 75, 26–39.

Ames 3rd, A., Li, Y.Y., Heher, E.C., Kimble, C.R., 1992. Energy metabolism of rabbit retina as related to function: high cost of Na+ transport. J. Neurosci. 12, 840–853.

Blenkinsop, T.A., Salero, E., Stern, J.H., Temple, S., 2013. The culture and maintenance of functional retinal pigment epithelial monolayers from adult human eye. Methods Mol. Biol. 945, 45–65.

Bok, D., 1993. The retinal pigment epithelium: a versatile partner in vision. J. Cell Sci. Suppl. 17, 189–195.

Bok, D., 2005. Evidence for an inflammatory process in age-related macular degeneration gains new support. Proc. Natl. Acad. Sci. U. S. A. 102, 7053–7054.

Bonilha, V.L., 2013 Sep 30. Retinal pigment epithelium (RPE) cytoskeleton in vivo and in vitro. Exp. Eye Res. pii: S0014-4835(13)00281-9. http://dx.doi.org/10.1016/j.exer.2013.09.015. (Epub ahead of print).

Chang, C., Wang, X., Caldwell, R.B., 1997a. Serum opens tight junctions and reduces ZO-1 protein in retinal epithelial cells. J. Neurochem. 69, 859–867.

Chang, C.W., Ye, L., Defoe, D.M., Caldwell, R.B., 1997b. Serum inhibits tight junction formation in cultured pigment epithelial cells. Investig. Ophthalmol. Vis. Sci. 38, 1082–1093.

Chew, E.C., Liew, C.T., Chew, S.B., Lee, J.C., Hou, H.J., Yam, H.F., Ho, P.C., Ip, S.M., 1993. The growth and behaviour of pig retinal pigment epithelial cells in culture. In vivo 7, 425–429.

Diemer, T., Gibbs, D., Williams, D.S., 2008. Analysis of the rate of disk membrane digestion by cultured RPE cells. Adv. Exp. Med. Biol. 613, 321–326.

Dintelmann, T.S., Heimann, K., Kayatz, P., Schraermeyer, U., 1999. Comparative study of ROS degradation by IPE and RPE cells in vitro. Graefes Arch. Clin. Exp. Ophthalmol. 237, 830–839.

Dithmer, M., Fuchs, S., Shi, Y., Schmidt, H., Richert, E., Roider, J., Klettner, A., 2014. Fucoidan reduces secretion and expression of vascular endothelial growth factor in the retinal pigment epithelium and reduces angiogenesis in vitro. PLoS One 9, e89150.

Drexler, H.G., Uphoff, C.C., 2002. Mycoplasma contamination of cell cultures: incidence, sources, effects, detection, elimination, prevention. Cytotechnology 39, 75–90.

Finnemann, S.C., Bonilha, V.L., Marmorstein, A.D., Rodriguez-Boulan, E., 1997. Phagocytosis of rod outer segments by retinal pigment epithelial cells requires alpha(v)beta5 integrin for binding but not for internalization. Proc. Natl. Acad. Sci. U. S. A. 94, 12932–12937.

Finnemann, S.C., Leung, L.W., Rodriguez-Boulan, E., 2002. The lipofuscin component A2E selectively inhibits phagolysosomal degradation of photoreceptor phospholipid by the retinal pigment epithelium. Proc. Natl. Acad. Sci. U. S. A. 99, 3842–3847.

Francis, P.J., Appukuttan, B., Simmons, E., Landauer, N., Stoddard, J., Hamon, S., Ott, J., Ferguson, B., Klein, M., Stout, J.T., Neuringer, M., 2008. Rhesus monkeys and humans share common susceptibility genes for age-related macular disease. Hum. Mol. Genet. 17, 2673–2680.

Fuhrmann, S., Zou, C., Levine, E.M., 2013. Retinal pigment epithelium development, plasticity, and tissue homeostasis. Exp. Eye Res..

Geisen, P., McColm, J.R., King, B.M., Hartnett, M.E., 2006. Characterization of barrier properties and inducible VEGF expression of several types of retinal pigment epithelium in medium-term culture. Curr. Eye Res. 31, 739–748.

Gibbs, D., Kitamoto, J., Williams, D.S., 2003. Abnormal phagocytosis by retinal pigmented epithelium that lacks myosin VIIa, the Usher syndrome 1B protein. Proc. Natl. Acad. Sci. U. S. A. 100, 6481–6486.

Gordiyenko, N.V., Fariss, R.N., Zhi, C., MacDonald, I.M., 2010. Silencing of the CHM gene alters phagocytic and secretory pathways in the retinal pigment epithelium. Investig. Ophthalmol. Vis. Sci. 51, 1143–1150.

Groenen, M.A., Archibald, A.L., Uenishi, H., Tuggle, C.K., Takeuchi, Y., Rothschild, M.F., Rogel-Gaillard, C., Park, C., Milan, D., Megens, H.J., Li, S., Larkin, D.M., Kim, H., Frantz, L.A., Caccamo, M., Ahn, H., Aken, B.L., Anselmo, A., Anthon, C., Auvil, L., Badaoui, B., Beattie, C.W., Bendixen, C., Berman, D., Blecha, F., Blomberg, J., Bolund, L., Bosse, M., Botti, S., Bujie, Z., Bystrom, M., Capitanu, B., Carvalho-Silva, D., Chardon, P., Chen, C., Cheng, R., Choi, S.H., Chow, W., Clark, R.C., Clee, C., Crooijmans, R.P., Dawson, H.D., Dehais, P., De Sapio, F., Dibbits, B., Drou, N., Du, Z.Q., Eversole, K., Fadista, J., Fairley, S., Faraut, T., Faulkner, G.J., Fowler, K.E., Fredholm, M., Fritz, E., Gilbert, J.G., Giuffra, E., Gorodkin, J., Griffin, D.K., Harrow, J.L., Hayward, A., Howe, K., Hu, Z.L., Humphray, S.J., Hunt, T., Hornshoj, H., Jeon, J.T., Jern, P., Jones, M., Jurka, J., Kanamori, H., Kapetanovic, R., Kim, J., Kim, J.H., Kim, K.W., Kim, T.H., Larson, G., Lee, K., Lee, K.T., Leggett, R., Lewin, H.A., Li, Y., Liu, W., Loveland, J.E., Lu, Y., Lunney, J.K., Ma, J., Madsen, O., Mann, K., Matthews, L., McLaren, S., Morozumi, T., Murtaugh, M.P., Narayan, J., Nguyen, D.T., Ni, P., Oh, S.J., Onteru, S., Panitz, F., Park, E.W., Park, H.S., Pascal, G., Paudel, Y., Perez-Enciso, M., Ramirez-Gonzalez, R., Reecy, J.M., Rodriguez-Zas, S., Rohrer, G.A., Rund, L., Sang, Y., Schachtschneider, K., Schraiber, J.G., Schwartz, J., Scobie, L., Scott, C., Searle, S., Servin, B., Southey, B.R., Sperber, G., Stadler, P., Sweedler, J.V., Tafer, H., Thomsen, B., Wali, R., Wang, J., Wang, J., White, S., Xu, X., Yerle, M., Zhang, G., Zhang, J., Zhang, J., Zhao, S., Rogers, J., Churcher, C., Schook, L.B., 2012. Analyses of pig genomes provide insight into porcine demography and evolution. Nature 491, 393–398.

Hamann, S., Kiilgaard, J.F., la Cour, M., Prause, J.U., Zeuthen, T., 2003. Cotransport of H+, lactate, and H_2O in porcine retinal pigment epithelial cells. Exp. Eye Res. 76, 493–504.

Hamel, C.P., Tsilou, E., Pfeffer, B.A., Hooks, J.J., Detrick, B., Redmond, T.M., 1993. Molecular cloning and expression of RPE65, a novel retinal pigment epithelium-specific microsomal protein that is post-transcriptionally regulated in vitro. J. Biol. Chem. 268, 15751–15757.

Hammer, M., Richter, S., Guehrs, K.H., Schweitzer, D., 2006. Retinal pigment epithelium cell damage by A2-E and its photo-derivatives. Mol. Vis. 12, 1348–1354.

Hu, J., Bok, D., 2001. A cell culture medium that supports the differentiation of human retinal pigment epithelium into functionally polarized monolayers. Mol. Vis. 7, 14–19.

Joffre, C., Leclere, L., Buteau, B., Martine, L., Cabaret, S., Malvitte, L., Acar, N., Lizard, G., Bron, A., Creuzot-Garcher, C., Bretillon, L., 2007. Oxysterols induced inflammation and oxidation in primary porcine retinal pigment epithelial cells. Curr. Eye Res. 32, 271–280.

Kaida, M., Cao, F., Skumatz, C.M., Irving, P.E., Burke, J.M., 2000. Time at confluence for human RPE cells: effects on the adherens junction and in vitro wound closure. Investig. Ophthalmol. Vis. Sci. 41, 3215–3224.

Keene, C.D., Cudaback, E., Li, X., Montine, K.S., Montine, T.J., 2011. Apolipoprotein E isoforms and regulation of the innate immune response in brain of patients with Alzheimer's disease. Curr. Opin. Neurobiol. 21, 920–928.

Kennedy, C.J., Rakoczy, P.E., Robertson, T.A., Papadimitriou, J.M., Constable, I.J., 1994. Kinetic studies on phagocytosis and lysosomal digestion of rod outer segments by human retinal pigment epithelial cells in vitro. Exp. Cell Res. 210, 209–214.

Kevany, B.M., Palczewski, K., 2010. Phagocytosis of retinal rod and cone photoreceptors. Physiology (Bethesda) 25, 8–15.

Klettner, A., Westhues, D., Lassen, J., Bartsch, S., Roider, J., 2013. Regulation of constitutive vascular endothelial growth factor secretion in retinal pigment epithelium/choroid organ cultures: p38, nuclear factor kappaB, and the vascular endothelial growth factor receptor-2/phosphatidylinositol 3 kinase pathway. Mol. Vis. 19, 281–291.

Lakkaraju, A., 2012. Endo-lysosome function in the retinal pigment epithelium in health and disease. Adv. Exp. Med. Biol. 723, 723–729.

Lakkaraju, A., Finnemann, S.C., Rodriguez-Boulan, E., 2007. The lipofuscin fluorophore A2E perturbs cholesterol metabolism in retinal pigment epithelial cells. Proc. Natl. Acad. Sci. U. S. A. 104, 11026–11031.

Lassota, N., Kiilgaard, J.F., Prause, J.U., Qvortrup, K., Scherfig, E., la Cour, M., 2007. Surgical induction of choroidal neovascularization in a porcine model. Graefes Arch. Clin. Exp. Ophthalmol. 245, 1189–1198.

Madara, J.L., 1998. Regulation of the movement of solutes across tight junctions. Annu. Rev. Physiol. 60, 143–159.

Mair, K.H., Sedlak, C., Kaser, T., Pasternak, A., Levast, B., Gerner, W., Saalmuller, A., Summerfield, A., Gerdts, V., Wilson, H.L., Meurens, F., 2014. The porcine innate immune system: an update. Dev. Comp. Immunol..

Maminishkis, A., Chen, S., Jalickee, S., Banzon, T., Shi, G., Wang, F.E., Ehalt, T., Hammer, J.A., Miller, S.S., 2006. Confluent monolayers of cultured human fetal retinal pigment epithelium exhibit morphology and physiology of native tissue. Investig. Ophthalmol. Vis. Sci. 47, 3612–3624.

Miura, Y., Klettner, A., Roider, J., 2010. VEGF antagonists decrease barrier function of retinal pigment epithelium in vitro: possible participation of intracellular glutathione. Investig. Ophthalmol. Vis. Sci. 51, 4848–4855.

Molday, R.S., Hicks, D., Molday, L., 1987. Peripherin. A rim-specific membrane protein of rod outer segment discs. Investig. Ophthalmol. Vis. Sci. 28, 50–61.

Muller, C., Mas Gomez, N., Ruth, P., Strauss, O., 2014. Ca1.3 L-type channels, maxiK Ca-dependent K channels and bestrophin-1 regulate rhythmic photoreceptor outer segment phagocytosis by retinal pigment epithelial cells. Cell. Signal. 26, 968–978.

Nandrot, E.F., Kim, Y., Brodie, S.E., Huang, X., Sheppard, D., Finnemann, S.C., 2004. Loss of synchronized retinal phagocytosis and age-related blindness in mice lacking alphavbeta5 integrin. J. Exp. Med. 200, 1539–1545.

Nishiyama, K., Sakaguchi, H., Hu, J.G., Bok, D., Hollyfield, J.G., 2002. Claudin localization in cilia of the retinal pigment epithelium. Anat. Rec. 267, 196–203.

Petters, R.M., Alexander, C.A., Wells, K.D., Collins, E.B., Sommer, J.R., Blanton, M.R., Rojas, G., Hao, Y., Flowers, W.L., Banin, E., Cideciyan, A.V., Jacobson, S.G., Wong, F., 1997. Genetically engineered large animal model for studying cone photoreceptor survival and degeneration in retinitis pigmentosa. Nat. Biotechnol. 15, 965–970.

Quinn, R.H., Miller, S.S., 1992. Ion transport mechanisms in native human retinal pigment epithelium. Investig. Ophthalmol. Vis. Sci. 33, 3513–3527.

Rattner, A., Nathans, J., 2006. Macular degeneration: recent advances and therapeutic opportunities. Nat. Rev. Neurosci. 7, 860–872.

Rizzolo, L.J., 1990. The distribution of Na+,K(+)-ATPase in the retinal pigmented epithelium from chicken embryo is polarized in vivo but not in primary cell culture. Exp. Eye Res. 51, 435–446.

Rizzolo, L.J., 2014. Barrier properties of cultured retinal pigment epithelium. Exp. Eye Res..
Ross, J.W., Fernandez de Castro, J.P., Zhao, J., Samuel, M., Walters, E., Rios, C., Bray-Ward, P., Jones, B.W., Marc, R.E., Wang, W., Zhou, L., Noel, J.M., McCall, M.A., DeMarco, P.J., Prather, R.S., Kaplan, H.J., 2012. Generation of an inbred miniature pig model of retinitis pigmentosa. Investig. Ophthalmol. Vis. Sci. 53, 501–507.
Sanchez, I., Martin, R., Ussa, F., Fernandez-Bueno, I., 2011. The parameters of the porcine eyeball. Graefes Arch. Clin. Exp. Ophthalmol. 249, 475–482.
Shaner, N.C., Steinbach, P.A., Tsien, R.Y., 2005. A guide to choosing fluorescent proteins. Nat. Methods 2, 905–909.
Shirasawa, M., Sonoda, S., Terasaki, H., Arimura, N., Otsuka, H., Yamashita, T., Uchino, E., Hisatomi, T., Ishibashi, T., Sakamoto, T., 2013. TNF-alpha disrupts morphologic and functional barrier properties of polarized retinal pigment epithelium. Exp. Eye Res. 110, 59–69.
Siliciano, J.D., Goodenough, D.A., 1988. Localization of the tight junction protein, ZO-1, is modulated by extracellular calcium and cell-cell contact in Madin-Darby canine kidney epithelial cells. J. Cell Biol. 107, 2389–2399.
Sommer, J.R., Estrada, J.L., Collins, E.B., Bedell, M., Alexander, C.A., Yang, Z., Hughes, G., Mir, B., Gilger, B.C., Grob, S., Wei, X., Piedrahita, J.A., Shaw, P.X., Petters, R.M., Zhang, K., 2011. Production of ELOVL4 transgenic pigs: a large animal model for Stargardt-like macular degeneration. Br. J. Ophthalmol. 95, 1749–1754.
Sonoda, S., Spee, C., Barron, E., Ryan, S.J., Kannan, R., Hinton, D.R., 2009. A protocol for the culture and differentiation of highly polarized human retinal pigment epithelial cells. Nat. Protoc. 4, 662–673.
Strauss, O., 2005. The retinal pigment epithelium in visual function. Physiol. Rev. 85, 845–881.
Terasaki, H., Kase, S., Shirasawa, M., Otsuka, H., Hisatomi, T., Sonoda, S., Ishida, S., Ishibashi, T., Sakamoto, T., 2013. TNF-alpha decreases VEGF secretion in highly polarized RPE cells but increases it in non-polarized RPE cells related to crosstalk between JNK and NF-kappaB pathways. PLoS One 8, e69994.
Tian, J., Ishibashi, K., Honda, S., Boylan, S.A., Hjelmeland, L.M., Handa, J.T., 2005. The expression of native and cultured human retinal pigment epithelial cells grown in different culture conditions. Br. J. Ophthalmol. 89, 1510–1517.
Xu, J., Toops, K.A., Diaz, F., Carvajal-Gonzalez, J.M., Gravotta, D., Mazzoni, F., Schreiner, R., Rodriguez-Boulan, E., Lakkaraju, A., 2012. Mechanism of polarized lysosome exocytosis in epithelial cells. J. Cell Sci. 125, 5937–5943.